Investigation of Water Structure at the TiO_2/Aqueous Interface

Sho Kataoka, Marc C. Gurau, Fernando Albertorio, Matthew A. Holden, Soon-Mi Lim, Richard D. Yang, and Paul S. Cremer*

Department of Chemistry, Texas A&M University, P.O. Box 30012, College Station, Texas 77842-3012

Received October 22, 2003. In Final Form: December 15, 2003

TiO_2 thin films coated on SiO_2 substrates were prepared for the investigation of water structure at the TiO_2/aqueous interface by vibrational sum-frequency spectroscopy (VSFS). The films were first characterized by X-ray photoelectron spectroscopy, ellipsometry, and atomic force microscopy. Film thickness could be readily varied between 0.9 and 5.9 nm with the thinnest film displaying the least degree of surface roughness. The 0.9 nm films were employed in the VSFS investigations and showed characteristic 3200 and 3400 cm^{-1} OH stretch frequencies of highly aligned interfacial water. Such peaks were reminiscent of those known from SiO_2/aqueous interfaces; however, the chemistry at TiO_2/aqueous interfaces was significantly richer. In the presence of Cl anions, the surface had an isoelectric point near pH 5.5 and showed the least degree of water organization near this pH. Almost equally strong 3200 cm^{-1} features could be produced at pH 2.0 and 12.0. On the other hand, the spectra were dramatically altered in the presence of phosphate-buffered saline. The phosphate ions specifically bound to the substrate surface and shifted the isoelectric point of the interface to pH 2.0. In this case, the intensity of the 3400 cm^{-1} peak was significantly increased in comparison with the Cl ion data at both neutral and acidic pH values. This is presumably because of a lack of sites directly adjacent to the oxide for forming tetrahedrally coordinated water when phosphate ions are present.

Introduction

Titanium dioxide (TiO_2) draws significant interest from researchers in a wide range of disciplines including catalysis, optics, and electrochemistry.[1−6] Additionally, titanium metal is commonly employed in artificial implants due to the biocompatibility of the thin TiO_2 layer at its surface.[7−12] Studies of TiO_2 interfaces, which are essential for understanding these applications, have greatly intensified with the development of modern analytical techniques such as scanning tunneling microscopy (STM),[4,13] atomic force microscopy (AFM),[14] X-ray photoelectron spectroscopy (XPS),[15] Fourier transform infrared (FTIR) spectroscopy,[16−18] and vibrational sum-frequency spectroscopy (VSFS).[19−21]

Of interest herein is the elucidation of water structure at the TiO_2/aqueous interface. Obtaining such information may ultimately prove crucial for understanding the adsorption, displacement, and spreading of protein molecules at nascently formed artificial/biological interfaces.[22,23] At present, little is known about the basic interfacial structure of water on titanium dioxide. In fact, the vast majority of VSFS studies of water structure at liquid/solid interfaces have been performed at the SiO_2/aqueous interface.[24−31] There are good reasons to suspect, however, that the behavior of water may be different on titanium dioxide surfaces. TiO_2 has its isoelectric point much closer to neutral pH in the presence of simple salt solutions than does SiO_2 (pH 5.5 vs 2.3),[32−37] and TiO_2

* To whom correspondence should be addressed. Tel: 979-862-1200. Fax: 979-845-7561. E-mail: cremer@mail.chem.tamu.edu.

(1) Wang, R.; Hashimoto, K.; Fujishima, A.; Chikuni, M.; Kojima, E.; et al. *Nature* **1997**, *388*, 431−432.
(2) Fujishim, A.; Honda, K. *Nature* **1972**, *238*, 37.
(3) Hoffmann, M. R.; Martin, S. T.; Choi, W. Y.; Bahnemann, D. W. *Chem. Rev.* **1995**, *95*, 69−96.
(4) Diebold, U. *Surf. Sci. Rep.* **2003**, *48*, 53−229.
(5) Gratzel, M. *Nature* **2003**, *421*, 586−587.
(6) Gratzel, M. *Nature* **1993**, *366*, 206−207.
(7) Areva, S.; Peltola, T.; Sailynoja, E.; Laajalehto, K.; Linden, M.; et al. *Chem. Mater.* **2002**, *14*, 1614−1621.
(8) Eriksson, C.; Lausmaa, J.; Nygren, H. *Biomaterials* **2001**, *22*, 1987−1996.
(9) Cacciafesta, P.; Humphris, A. D. L.; Jandt, K. D.; Miles, M. J. *Langmuir* **2000**, *16*, 8167−8175.
(10) Bentaleb, A.; Abele, A.; Haikel, Y.; Schaaf, P.; Voegel, J. C. *Langmuir* **1998**, *14*, 6493−6500.
(11) Masuda, Y.; Ieda, S.; Koumoto, K. *Langmuir* **2003**, *19*, 4415−4419.
(12) Kilpadi, D. V.; Raikar, G. N.; Liu, J.; Lemons, J. E.; Vohra, Y.; et al. *J. Biomed. Mater. Res.* **1998**, *40*, 646−659.
(13) Henderson, M. A. *Surf. Sci. Rep.* **2002**, *46*, 5−308.
(14) Tanaka, H.; Tabata, N.; Kawai, T. *Thin Solid Films* **1999**, *342*, 4−7.
(15) Chusuei, C. C.; Goodman, D. W.; Van Stipdonk, M. J.; Justes, D. R.; Loh, K. H.; et al. *Langmuir* **1999**, *15*, 7355−7360.
(16) Connor, P. A.; Dobson, K. D.; McQuillan, A. J. *Langmuir* **1999**, *15*, 2402−2408.
(17) Connor, P. A.; Dobson, K. D.; McQuillan, A. J. *Langmuir* **1995**, *11*, 4193−4195.
(18) Roddick-Lanzilotta, A. D.; Connor, P. A.; McQuillan, A. J. *Langmuir* **1998**, *14*, 6479−6484.
(19) Miyamae, T.; Yamada, Y.; Uyama, H.; Nozoye, H. *Surf. Sci.* **2001**, *493*, 314−318.
(20) Miyamae, T.; Nozoye, H. *J. Photochem. Photobiol., A* **2001**, *145*, 93−99.
(21) Wang, C. Y.; Groenzin, H.; Shultz, M. J. *Langmuir* **2003**, *19*, 7330−7334.
(22) Vogler, E. A. *Adv. Colloid Interface Sci.* **1998**, *74*, 69−117.
(23) Israelachvili, J.; Wennerstrom, H. *Nature* **1996**, *379*, 219−225.
(24) Du, Q.; Freysz, E.; Shen, Y. R. *Science* **1994**, *264*, 826−828.
(25) Du, Q.; Freysz, E.; Shen, Y. R. *Phys. Rev. Lett.* **1994**, *72*, 238−241.
(26) Shen, Y. R. *Nature* **1989**, *337*, 519−525.
(27) Shen, Y. R. *Solid State Commun.* **1998**, *108*, 399−406.
(28) Kim, J.; Cremer, P. S. *J. Am. Chem. Soc.* **2000**, *122*, 12371−12372.
(29) Kim, J.; Cremer, P. S. *ChemPhysChem* **2001**, *2*, 543.
(30) Kim, J.; Kim, G.; Cremer, P. S. *Langmuir* **2001**, *17*, 7255−7260.
(31) Kim, J.; Kim, G.; Cremer, P. S. *J. Am. Chem. Soc.* **2002**, *124*, 8751−8756.
(32) Nelson, B. P.; Candal, R.; Corn, R. M.; Anderson, M. A. *Langmuir* **2000**, *16*, 6094−6101.
(33) Yezek, L.; Rowell, R. L.; Larwa, M.; Chibowski, E. *Colloids Surf., A* **1998**, *141*, 67−72.
(34) Fairhurst, A. J.; Warwick, P.; Richardson, S. *Colloids Surf., A* **1995**, *99*, 187−199.

10.1021/la035971h CCC: $27.50
Published on Web 01/22/2004

becomes positively charged below pH 5.5. Also, TiO_2 can specifically adsorb certain inorganic anions such as phosphate, which significantly shift the isoelectric point at the interface.[32,38] SiO_2, which has an isoelectric point near pH 2.3, does not seem to display similar behavior.[39]

VSFS has recently grown to be a powerful source of surface specific vibrational information under ambient conditions. The basic principles have been discussed elsewhere.[24−27,40−43] Briefly, VSFS provides vibrational information on molecules at interfaces even in the presence of an overwhelming bulk contribution. As an optical technique, it has been exploited for investigating vapor/liquid, solid/liquid, and liquid/liquid interfaces. While VSFS has yet to be applied to the TiO_2/aqueous interface, studies have been conducted at other solid/aqueous interfaces including the SiO_2/water,[24−27] Al_2O_3/water,[44] and CaF_2/water interfaces.[45,46] TiO_2/aqueous interfaces have been observed, however, by second harmonic generation (SHG).[47,48] Furthermore, a catechol complex has been made on colloidal TiO_2 particles and a surface charge-transfer process was directly observed by SHG in aqueous solution in its presence.[49,50] In terms of nonaqueous titanium dioxide interfaces, VSFS has recently been exploited for investigating the photocatalytic reaction of poly(ethylene terephthalate) on TiO_2.[20] Also, the presence of trace hydrocarbon species has been monitored on nanoparticulate TiO_2 surfaces in the presence and absence of UV illumination.[21]

Herein we report on the preparation and investigation of ultrathin TiO_2 films on SiO_2 substrates. The surfaces were characterized by AFM, XPS, and ellipsometry. VSFS data were collected at the TiO_2/aqueous interface in the presence of chloride and phosphate anions over a range of pH values. The results are directly compared to the SiO_2/aqueous interface. The data reveal that water structure at titanium dioxide is highly dependent upon both the pH of the aqueous solution and the specific nature of the anions present.

Experimental Section

TiO_2 Thin Film Preparation and Characterization. Recently, several methods have been developed for the preparation of TiO_2 thin films.[11,51−54] These were modified to fit the present studies as follows: round SiO_2 substrates (1 in. diameter, 1/8 in. thick IR grade fused quartz; Quartz Plus Inc., Brookline, NH) were cleaned and subsequently annealed in a kiln at 500 °C for 6 h. Each disk was then soaked in concentrated sulfuric acid (EM Science, Gibbstown, NJ) for 5 h followed by rinsing with copious amounts of water and methanol in order to hydroxylate the interface. Next, the disks were exposed to titanium(IV) isopropoxide ($Ti(O^iPr)_4$; Aldrich, Milwaukee, WI) in a closed environment for time periods ranging from 10 to 120 min at room temperature (see Figure 1), which allowed $Ti(O^iPr)_4$ vapor (vapor pressure, 10 mmHg at 14 °C) to react with the surface silanol groups. The time period of exposure dictated the ultimate thickness of the film that could be achieved. Afterward, the disks were washed with water and acetone before a final calcination at 500 °C for 6 h.

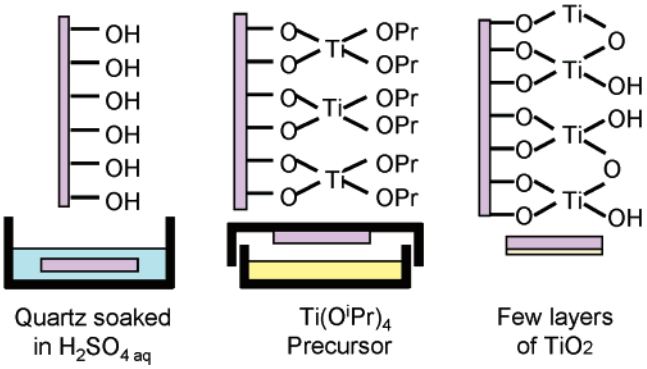

Figure 1. Schematic diagram of the preparation of TiO_2 thin films on a SiO_2 disk: (left) a SiO_2 disk was hydroxylated with H_2SO_4, (middle) then exposed to the $Ti(O^iPr)_4$ precursor in a Petri dish, and (right) finally washed with water and acetone to remove excess isopropoxide.

The TiO_2 films were characterized by XPS to determinate their chemical composition. Ellipsometry measurements were made to access film thickness, and AFM was performed to provide topographical information about film roughness. The XPS spectra were obtained using monochromatic Al Kα radiation, operating at 15 kV and 15 mA (AXIS His 165 and Ultra; Kratos Analytical Ltd., Manchester, U.K.). Survey scans were obtained over a range of binding energies from 0 to 1000 eV, from which the atomic fractions of Ti and Si were determined. High-resolution scans for Ti 2p and O 1s were acquired in order to ascertain the oxidation state of the titanium. The peak positions were corrected using the binding energy of the C 1s peak at 284.8 eV as a reference. Subsequently, film thickness was measured with an ellipsometer (model L2W26D; Gaertner Scientific, Skokie, IL) employing a laser beam at 632 nm and an angle of incidence set at 80°. An index of refraction of 2.46 was assumed for these measurements.[55,56] Finally, to determine the surface roughness and topography, tapping-mode AFM images were obtained with a Nanoscope IIIa Multimode SPM (Digital Instruments, Santa Barbara, CA) equipped with a J-type scanner and a crystalline silicon probe tip (125 μm, 300 kHz response frequency).

VSFS Experiments. VSFS is a second-order nonlinear optical spectroscopy whereby two incident laser beams (variable frequency infrared and fixed frequency visible) are overlapped at an interface to generate an output at the sum of the two frequencies.[26,27,40,42] This process is forbidden in the dipole approximation in bulk centrosymmetric media. Only highly aligned oscillators at the surface of such systems give rise to signal where inversion symmetry is necessarily broken.

VSFS experiments were performed with a mode-locked Nd:YAG laser (PY61c; Continuum, Santa Clara, CA) operated at a 20 Hz repetition rate with a temporal peak width of 21 ps.[28−31] The laser beam, which had a wavelength of 1064 nm, was sent

(35) Moser, J.; Punchihewa, S.; Infelta, P. P.; Gratzel, M. *Langmuir* **1991**, *7*, 3012−3018.
(36) Morris, G. E.; Skinner, W. A.; Self, P. G.; Smart, R. S. *Colloids Surf., A* **1999**, *155*, 27−41.
(37) Venz, P. A.; Frost, R. L.; Kloprogge, J. T. *J. Non-Cryst. Solids* **2000**, *276*, 95−112.
(38) Kazarinov, V. E.; Andreev, V. N.; Mayorov, A. P. *J. Electroanal. Chem.* **1981**, *130*, 277−285.
(39) Coreno, J.; Martinez, A.; Bolarin, A.; Sanchez, F. *J. Biomed. Mater. Res.* **2001**, *57*, 119−125.
(40) Watry, M. R.; Brown, M. G.; Richmond, G. L. *Appl. Spectrosc.* **2001**, *55*, 321A−340A.
(41) Richmond, G. L. *Annu. Rev. Phys. Chem.* **2001**, *52*, 357−389.
(42) Richmond, G. L. *Chem. Rev.* **2002**, *102*, 2693−2724.
(43) Brown, M. G.; Raymond, E. A.; Allen, H. C.; Scatena, L. F.; Richmond, G. L. *J. Phys. Chem. A* **2000**, *104*, 10220−10226.
(44) Yeganeh, M. S.; Dougal, S. M.; Pink, H. S. *Phys. Rev. Lett.* **1999**, *83*, 1179−1182.
(45) Becraft, K. A.; Moore, F. G.; Richmond, G. L. *J. Phys. Chem. B* **2003**, *107*, 3675−3678.
(46) Becraft, K. A.; Richmond, G. L. *Langmuir* **2001**, *17*, 7721−7724.
(47) Kobayashi, E.; Matsuda, K.; Mizutani, G.; Ushioda, S. *Surf. Sci.* **1999**, *428*, 294−297.
(48) Mizutani, G.; Ishibashi, N.; Nakamura, S.; Sekiya, T.; Kurita, S. *Int. J. Mod. Phys. B* **2001**, *15*, 3873−3876.
(49) Liu, Y.; Dadap, J. I.; Zimdars, D.; Eisenthal, K. B. *J. Phys. Chem. B* **1999**, *103*, 2480−2486.
(50) Eisenthal, K. B. *J. Phys. Chem.* **1996**, *100*, 12997−13006.
(51) Ichinose, I.; Takaki, R.; Kuroiwa, K.; Kunitake, T. *Langmuir* **2003**, *19*, 3883−3888.
(52) Fadeev, A. Y.; McCarthy, T. J. *J. Am. Chem. Soc.* **1999**, *121*, 12184−12185.
(53) Fadeev, A. Y.; McCarthy, T. J. *Langmuir* **1999**, *15*, 7238−7243.
(54) Fadeev, A. Y.; McCarthy, T. J. *Langmuir* **1999**, *15*, 3759−3766.
(55) Remillard, J. T.; McBride, J. R.; Nietering, K. E.; Drews, A. R.; Zhang, X. *J. Phys. Chem. B* **2000**, *104*, 4440−4447.
(56) Alvarez-Herrero, A.; Fort, A. J.; Guerrero, H.; Bernabeu, E. *Thin Solid Films* **1999**, *349*, 212−219.

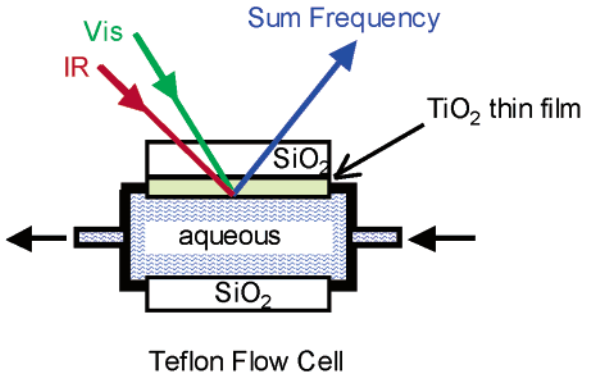

Figure 2. Schematic side-cut view of the flow cell showing beams for VSFS measurements.

through an optical parametric generation/amplification (OPG/OPA) stage (Laser Vision, Bellevue, WA) to produce a tunable IR beam between 2700 and 3700 cm^{-1} as well as fixed frequency radiation at 532 nm. The polarization combination used in these experiments was SSP, referring to the sum frequency, visible, and infrared beams, respectively.

The experimental setup, including a homemade Teflon flow cell for taking data, has been described in previous publications.[28−31] A TiO_2-coated SiO_2 disk was fitted onto the cell so that the coated side faced inward toward the water solution (Figure 2). The input laser beams were transmitted through the coated substrate and focused at the TiO_2/aqueous interface. All aqueous solutions were prepared with water obtained from a NANOpure Ultrapure Water System (Barnstead, Dubuque, IA). Several solutions at various pH values (2.0, 4.0, 6.0, 8.0, 10.0, and 12.0) were flowed through the system. The pH of the solutions was controlled by the addition of either NaOH or HCl (EM Science), while the total ionic strength of a given solution was maintained at 30 mM by the addition of NaCl (EM Science). Additional data were taken in the presence of phosphate ions. In this case, 30 mM phosphate-buffered saline (PBS) solutions were prepared using the appropriate quantity of sodium phosphate with the addition of NaOH or HCl to control the pH. The spectra collected at each pH value were averaged and normalized to spectra taken from a piece of Y-cut crystalline quartz.

Results and Discussion

Film Preparation and Characterization. After deposition of a titanium dioxide film onto a SiO_2 substrate, XPS was used to characterize the chemical composition of the surface. Figure 3 shows both a survey and a high-resolution XPS spectrum for a TiO_2 film made from a 10 min exposure to the $Ti(O^iPr)_4$ precursor. The survey scan contained noticeable peaks for Ti, O, C, and Si. The Ti $2p_{3/2}$ and $2p_{1/2}$ peaks had binding energies of 458.9 and 465.0 eV, which are expected for Ti existing in the form of TiO_2.[12] The atomic fractions of all elements were constant over different regions of the film at least down to the size of the X-ray beam spot profile (200 × 200 μm^2). As noted, the XPS survey spectrum contained a small but noticeable carbon peak (C 1s), which is believed to arise from atmospheric exposure of the film rather than as a consequence of the use of the $Ti(O^iPr)_4$ precursor since the organic should be completely oxidized to carbon dioxide during the film calcination process.

The thickness of the TiO_2 films varied with the amount of time a given disk was exposed to $Ti(O^iPr)_4$. The results of ellipsometric measurements are shown as a function of the exposure time, along with the atomic fraction of Si and Ti obtained from the XPS spectra (Figure 4). The film thickness increased roughly linearly with increasing exposure time. As expected, the atomic fraction of Si detected by XPS was highest for the thinnest film and decreased with film thickness. On the other hand, Ti

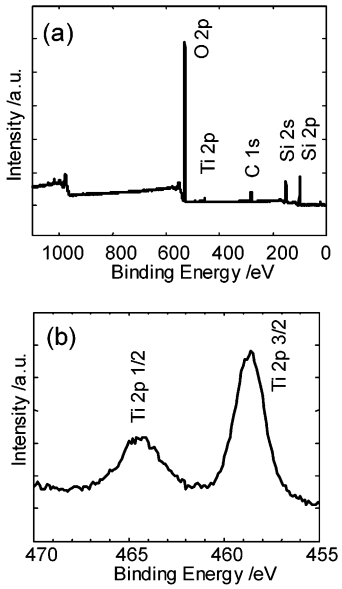

Figure 3. XPS spectra of a 0.9 nm thick TiO_2 film on a SiO_2 disk: (a) survey scan and (b) in the Ti 2p region.

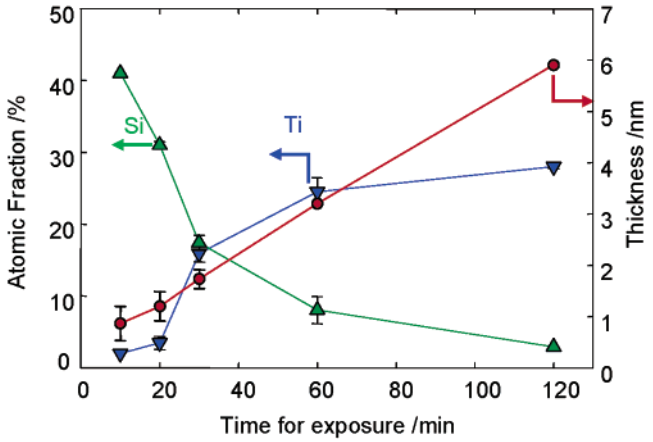

Figure 4. The atomic fractions of Ti (▼) and Si (▲) in TiO_2 thin films as well as the TiO_2 layer thickness (●) as a function of the exposure time to the $Ti(O^iPr)_4$ precursor.

showed the opposite behavior. The Si peak is expected to be present for all exposure times even for uniformly covered surfaces since the escape depth of the photoelectrons is at least as large as the thickness of the films in the present study.[57]

The films were next characterized by AFM. Figure 5 shows images taken of (a) a bare SiO_2 disk, (b) a 0.9 nm film, (c) a 1.6 nm film, and (d) a 3.2 nm film. All images were acquired in tapping mode with a scan area of 200 × 200 nm^2. The 0.9 nm thick TiO_2 film was not noticeably rougher than the one obtained from bare SiO_2, indicating that no "islandlike" film deposition occurred. Indeed, the root-mean-square (rms) roughness of the film was 0.057 nm over a 200 × 200 nm^2 scan area as compared to 0.055 nm for bare SiO_2. The surface became somewhat rougher for the thicker films: the rms roughness was 0.128 nm for the 1.6 nm film and 0.172 nm for the 3.2 nm film. These are still rather smooth films; however, the increase may reflect an insufficient number of OH termini on top of the growing TiO_2 film. This in turn may limit subsequent uniform attack by the $Ti(O^iPr)_4$ precursor from the vapor phase. No particulate deposition was detected for any of

(57) Cappello, G.; Chevrier, J.; Schmithusen, F.; Stierle, A.; Formoso, V.; et al. *Phys. Rev. B* **2002**, *65*.

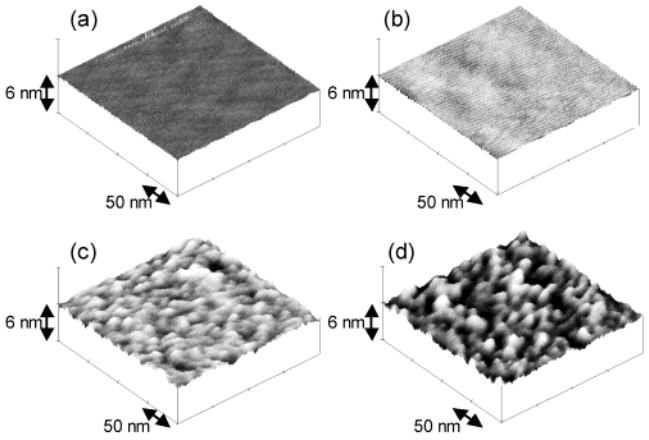

Figure 5. AFM images of TiO_2 thin films on a SiO_2 disk over a 200 × 200 nm^2 region: (a) a bare SiO_2 surface, (b) a 0.9 nm film, (c) a 1.6 nm film, and (d) a 3.2 nm film.

the films. Based on the above ellipsometry, XPS, and AFM results, it is reasonable to conclude that the TiO_2 film covered the vast majority of the SiO_2 substrates. Indeed, even the thinnest film showed little evidence for nonuniform surface coverage over scales ranging from hundreds of microns (XPS) to nearly one nanometer (AFM).

VSFS Spectra: pH Effects. Because of its relative smoothness and good uniformity, the 0.9 nm film was employed in the VSFS experiments presented below.[58] All VSFS investigations were undertaken at both the SiO_2/aqueous and TiO_2/aqueous interfaces. For reference, VSFS data were recorded between 2700 and 3700 cm^{-1} at the bare SiO_2/aqueous interface over a pH range from 2.0 to 12.0. The results are shown in Figure 6a. The spectra were dominated by two broad and prominent features at 3200 and 3400 cm^{-1}, consistent with previous studies of this interface.[24−26,41−43,59−61] The 3200 cm^{-1} peak is indicative of water with tetrahedral bonding. Its strength is largely determined by the magnitude of the electric field emanating from the negatively charged deprotonated silanols at the interface. The strength of this peak increases almost monotonically as the bulk pH is raised because a continually greater fraction of the silanols become deprotonated.[24,25,31,42] On the other hand, the 3400 cm^{-1} feature is produced by water molecules with less ordered hydrogen bonds. This peak emanates from species directly adjacent to the SiO_2 surface.[62,63] On the other hand, the 3200 cm^{-1} peak comes mostly from water molecules in subsequent layers; however, the 3200 cm^{-1} signal can arise from the first interfacial layer when the surface registry of silanols is appropriate to support some tetrahedral coordination.

VSFS data taken from the TiO_2/aqueous interface are shown in Figure 6b. Like the SiO_2 interface, the strength of the 3200 cm^{-1} peak increased above pH 6.0 and was accompanied by a comparable 3400 cm^{-1} peak. However,

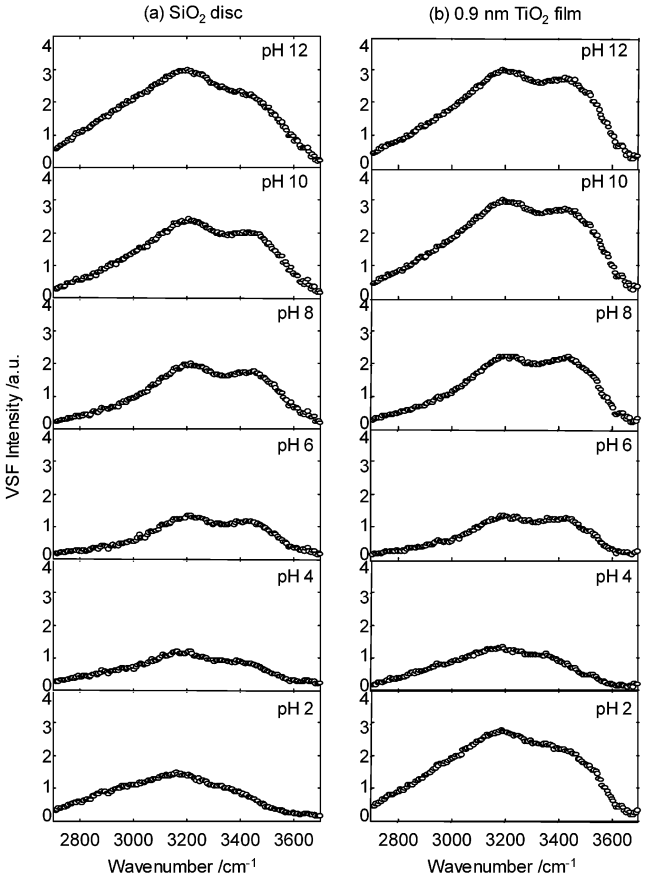

Figure 6. VSFS spectra of (a) the SiO_2/aqueous and (b) TiO_2/aqueous interfaces as a function of pH. Solutions were made with only HCl, NaOH, and NaCl.

the strength of these features reached a minimum near pH 4.0 and 6.0. It then showed a marked increase as the pH was lowered to 2.0. This increase in VSFS intensity under acidic conditions stems directly from the nature of TiO_2 surface chemistry. The TiO_2 interfacial layer is hydroxylated (i.e., forms Ti−OH) in a manner analogous to silanol formation on SiO_2;[39,44,64] however, the Ti−OH groups, which have an isoelectric point around pH 5.5 based on zeta potential measurements,[32−37] become positively charged under more acidic conditions. This behavior is in contrast to that of SiO_2, which only reaches its isoelectric point near pH 2.3.[39] In the case of TiO_2, there is probably a mixture of TiO^-, TiOH, and $TiOH_2^+$ moieties that exist near the isoelectric point and this interface becomes continuously more positively charged as the pH is lowered.[37] Since the sign of the charge of the TiO_2/aqueous interface changes as the pH is lowered through the isoelectric point, the water dipoles almost certainly flip as a result.[27] In other words, the oxygen end of the water molecules most likely points downward at low pH, while the protons face the surface under basic conditions.

VSFS Spectra: Phosphate Ion Effects. In the next set of experiments, phosphate-buffered saline was introduced at the SiO_2/aqueous and TiO_2/aqueous interfaces. In this case, 30 mM PBS was employed and the pH was adjusted to the desired value. Spectra for the SiO_2/aqueous interface between pH 2.0 and 12.0 are shown in Figure 7a. The intensity and width of the 3200 and 3400 cm^{-1} peaks are almost identical to those shown in Figure 6a, and the presence of phosphate ions in the buffer seems to

(58) Thicker films were also investigated but showed evidence for interference fringes that increased with layer thickness. Also, there was evidence for aligned water trapped beneath the surface of thicker films that could not be readily exchanged away by D_2O. These films are, therefore, not discussed further herein.

(59) Scatena, L. F.; Brown, M. G.; Richmond, G. L. *Science* **2001**, *292*, 908−912.

(60) Wei, X.; Miranda, P. B.; Shen, Y. R. *Phys. Rev. Lett.* **2001**, *86*, 1554−1557.

(61) Wei, X.; Miranda, P. B.; Zhang, C.; Shen, Y. R. *Phys. Rev. B* **2002**, *66*, art. no.-085401.

(62) Miranda, P. B.; Du, Q.; Shen, Y. R. *Chem. Phys. Lett.* **1998**, *286*, 1−8.

(63) Gurau, M. C.; Kim, G.; Lim, S. M.; Albertorio, F.; Fleisher, H. C.; Cremer, P. S. *ChemPhysChem* **2003**, *4*, 1231−1233.

(64) Coreno, J.; Martinez, A.; Coreno, O.; Bolarin, A.; Sanchez, F. *J. Biomed. Mater. Res., Part A* **2003**, *64A*, 131−137.

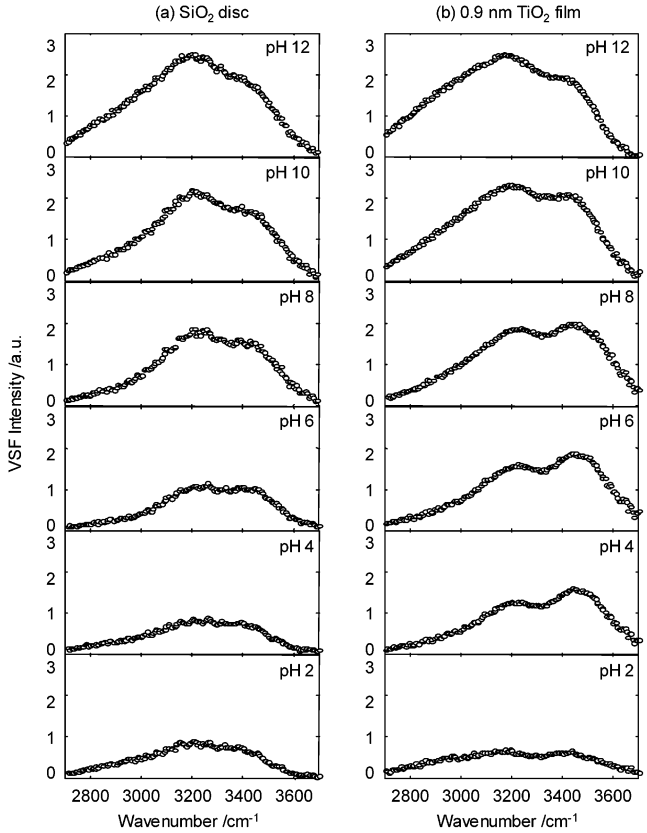

Figure 7. VSFS of (a) the SiO_2/aqueous and (b) the TiO_2/aqueous interfaces as a function of pH in PBS solutions.

have had little if any effect on the spectra. On the other hand, the sodium phosphate buffers had a profound effect at the TiO_2/aqueous interface (Figure 7b). In this case, the behavior of the 3200 cm^{-1} feature was quite different as a function of pH from solutions containing only chloride anions (Figure 6b). Specifically, no evidence was seen for an increase in this feature as the pH was brought down into the acidic range. In fact, the intensity of the 3200 cm^{-1} peak was quite small at pH 2.0 relative to more basic conditions.

Phosphate ions are known to strongly adsorb to TiO_2 surfaces and form bridged bidentate complexes.[64,65] Recently, Nelson and co-workers have measured the zeta potential of particulate TiO_2 in the presence and the absence of phosphate ions.[32] In their study, the isoelectric point of the surface of TiO_2 was shifted to pH 2 in the presence of 1 mM phosphate and little evidence was noted for the surface becoming positively charged below this value. Such zeta potential results in combination with the present VSFS data provide strong evidence that phosphate can specifically adsorb to TiO_2 and almost certainly resides in the inner Helmholtz plane.[66]

One curious finding in our TiO_2/PBS solution studies is that the 3400 cm^{-1} feature is strengthened by the presence of phosphate ions relative to the 3200 cm^{-1} peak. This was especially noticeable at pH values of 8.0 and below. The presence of adsorbed phosphate ions will alter the distances between hydrogen bond donor/acceptor sites at the TiO_2 surface. From the data, it can be inferred that the phosphate adsorbate makes it more difficult to obtain the requisite registry for tetrahedral water coordination in the first water monolayer. This causes an increase in the number of water molecules directly adjacent to the interface without a full complement of hydrogen bonds and hence increases the 3400 cm^{-1} signal.

Outlook. Investigations of water structure at the TiO_2/aqueous interface clearly demonstrate some similarities and some differences of this oxide with silica. The door is now open to exploring TiO_2 films in the presence of various polymer, protein, and surfactant adsorbates. A key question for future studies will be to ascertain whether the molecular level details of water organization can be correlated with biofouling processes. This is especially important in light of the fact that TiO_2 can be used in implants. From a molecular point of view, it will be key to determine if water molecules either directly adjacent to the substrate (associated with the 3400 cm^{-1} peak) or those aligned by the interfacial electric field (associated with the 3200 cm^{-1} peak) can signify resistance or enhancement of macromolecular adsorption.

Conclusions

Herein we have developed a simple procedure for creating TiO_2 ultrathin films on SiO_2 substrates suitable for the investigation of water structure using VSFS. Characterization of these films by XPS, ellipsometry, and AFM suggested that 0.9 nm thick films were uniform both chemically and topologically. The method could be used to control layer thickness, although thicker films suffered from slightly greater roughness. VSFS spectra of films at the solid/aqueous interface revealed the presence of ordered water structure reminiscent of that seen from the SiO_2/aqueous interface. The TiO_2 films, however, proved to have far richer chemistry. In the presence of simple salt solutions (NaCl), the water peaks displayed a minimum in intensity near pH 4.0 and 6.0. This is quite close to the system's known isoelectric point of pH 5.5. The intensity of the 3200 cm^{-1} feature was dramatically increased at pH values above and below this point. On the other hand, adding phosphate anions to the solution shifted the isoelectric point down near pH 2.0 due to their strong adsorption on the surface of TiO_2. This caused the 3200 cm^{-1} peak intensity to obey roughly the same behavior as a function of pH as that seen at the SiO_2/aqueous interface. The 3400 cm^{-1} peak was strengthened in relation to the 3200 cm^{-1} feature by the presence of phosphate ions.

Acknowledgment. This work was funded by the National Science Foundation (CHE-0094332) and the Robert A. Welch Foundation (Grant A-1421). P.S.C. gratefully acknowledges the Sloan Foundation, the Beckman Foundation, and the Dreyfus Foundation for additional fellowship support. We also acknowledge Professor Richard M. Crooks for the use of his ellipsometer and Dr. Yulia Vasilyeva in the Center for Integrated Microchemical Systems at Texas A&M University for help with AFM measurements.

LA035971H

(65) Ronson, T. K.; McQuillan, A. J. *Langmuir* **2002**, *18*, 5019−5022.
(66) Hunter, R. J.; Ottewill, R. H. *Zeta potential in colloid science*: *Principles and applications*; Academic Press: London, 1981.